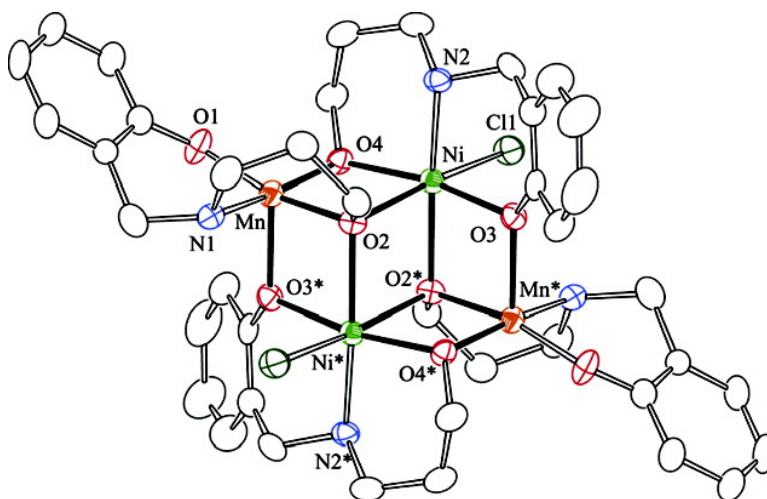Communication

A Heterometal Single-Molecule Magnet of [MnNiCl(salpa)]

Hiroki Oshio, Masayuki Nihei, Satoshi Koizumi, Takuya Shiga, Hiroyuki
Nojiri, Motohiro Nakano, Naoki Shirakawa, and Mitsuhiro Akatsu

More About This Article

Additional resources and features associated with this article are available within the HTML version:

- Supporting Information
- Links to the 15 articles that cite this article, as of the time of this article download
- Access to high resolution figures
- Links to articles and content related to this article
- Copyright permission to reproduce figures and/or text from this article

View the Full Text HTML

A Heterometal Single-Molecule Magnet of [Mn$^{III}_2$Ni$^{II}_2$Cl$_2$(salpa)$_2$]

Hiroki Oshio,*,† Masayuki Nihei,† Satoshi Koizumi,† Takuya Shiga,† Hiroyuki Nojiri,‡
Motohiro Nakano,¶ Naoki Shirakawa,§ and Mitsuhiro Akatsu§

*Department of Chemistry, Graduate School of Pure and Applied Sciences, University of Tsukuba, Tennodai 1-1-1,
Tsukuba 305-8571, Japan, Institute of Material Research, Tohoku University, Katahira 2-1-1,
Aoba-ku, Sendai 980-8577, Japan, Department of Molecular Chemistry, Graduate School of Engineering, Osaka
University, 1-16 Machikaneyama, Toyonaka, Osaka 560-0043, Japan, and Nanoelectronics Research Institute,
National Institute of Advanced Industrial Science and Technology, Tsukuba Central 1, Tsukuba 305-8561 Japan*

Received December 27, 2004; E-mail: oshio@chem.tsukuba.ac.jp

High-spin molecules with an easy-axis magnetic anisotropy show slow magnetic relaxation of the spin reorientation along the magnetic anisotropy axis, and at very low temperature, the spin does not thermally flip but flips via quantum processes. These molecules have a double minimum potential for the reversal of the magnetic moment and are called single-molecule magnets (SMMs).[1] SMMs, which have possible applications as very small memory devices, are fundamentally interesting due to quantum phenomena for future applications in quantum computing.[2] Since the discovery of the first SMM of a dodecanuclear manganese complex,[3] many homometal SMMs composed of V, Mn, Fe, and Ni ions have been prepared,[4] and their quantum behaviors have been extensively studied.[5] By combining different metal ions, on the other hand, it should be possible to prepare molecules with larger magnetic anisotropy and higher spin ground states due to ferro- or antiferromagnetic interactions. Today, the number of heterometal SMMs is still limited,[6] even though SMMs will lead to an understanding of quantum tunneling effects through synergy of heterometal spins. We report here a new heterometal SMM of [Mn$^{III}_2$Ni$^{II}_2$Cl$_2$(salpa)$_2$] (salpa = N-(2-hydroxybenzyl)-3-amino-1-propanol), which showed a steplike hysteresis loop characteristic of an SMM.

A reaction of 1:1 mixtures of H$_2$salpa[7] and metal chlorides in methanol gave dark-red crystals of [Mn$^{III}_2$Ni$^{II}_2$Cl$_2$(salpa)$_2$] (**1**) in a high yield (40%).[8] **1** crystallized in a tetragonal space group of $I4_1/a$.[9] The structure consists of an incomplete face-sharing double cube that is composed of two Mn^{III} and two Ni^{II} ions (Figure 1). Metal ion positions were confirmed by bond valence sum calculations[10] and the short coordination bond lengths for the Mn^{III} ions. The Mn^{III} and Ni^{II} ions are doubly bridged to form a dinuclear unit by two oxygen atoms (O4 and O2), and the symmetrically related dinuclear cores are linked by two phenoxo (O3 and O3*) and two alkoxo (O2 and O2*) groups in μ_2 and μ_3 fashions, respectively. The Mn^{III} ion has square pyramidal coordination geometry. The equatorial positions are occupied by three oxygen (O1, O4, and O2) and one nitrogen (N1) atoms, and a phenoxo oxygen atom (O3*) coordinates from the apical position. The Ni^{II} ion has an N$_1$O$_4$Cl$_1$ chromophore, and the coordination bond lengths of the Ni^{II} ion are longer than those of the Mn^{III} ion. The Ni^{II} ions are separated by 3.101(2) Å, and interatomic distance of the Mn^{III} and Ni^{II} is 3.065(2) Å.

DC magnetic susceptibility measurements for **1** were performed in the temperature range from 1.8 to 300 K (Figure 2). The $\chi_m T$ value at 300 K is 8.768 emu mol^{-1} K, which is somewhat larger than the value of the Curie constant (8.00 emu mol^{-1} K with $g =$

† University of Tsukuba.
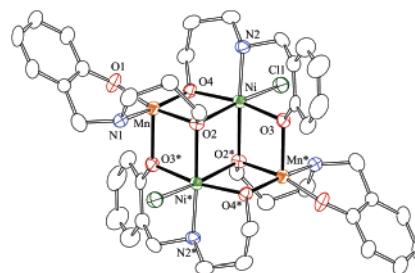‡ Tohoku University.
¶ Osaka University.
§ AIST.

Figure 1. ORTEP diagram of **1**. Selected bond angles (deg): Mn−O2−Ni 97.3(2), Mn−O2−Ni* 95.4(2), Ni−O2−Ni* 101.65(19), Ni−O3−Mn* 98.5(2), Mn−O4−Ni 103.3(2).
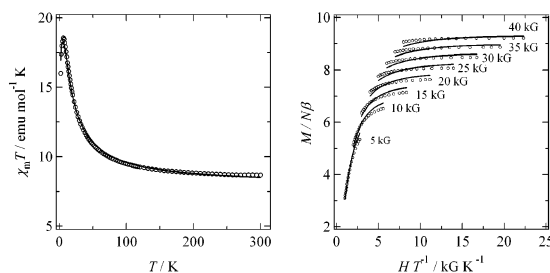

Figure 2. $\chi_m T$ versus T (left) plot and field dependence of magnetization at the field indicated (right) for **1**. The solid lines are the best fits using the values in the text.

2) for the uncorrelated Mn^{III} and Ni^{II} ions. The $\chi_m T$ values gradually increased as the temperature was decreased and reached a maximum value (18.56 emu mol^{-1} K) at 6.0 K, followed by sudden decrease. The magnetic susceptibility data indicate that the molecule has a relatively large spin ground state, such as $S = 5$ and 6, of which Curie constants are 15 and 21 emu mol^{-1} K, respectively. Magnetization data were collected as a function of the temperature and applied magnetic field (Figure 1S in the Supporting Information). The magnetic susceptibility and low-temperature magnetization data for the powder sample were simultaneously analyzed by using a Heisenberg−Dirac−Van Vleck spin Hamiltonian,[11] where three exchange coupling constants (J_{MnNi}, J_{MnNi*}, and J_{NiNi*}) and uniaxial zero-field splitting parameters were assumed and constant values of TIP (50 × 10^{-6} and 240 × 10^{-6} emu per Mn and Ni ions, respectively) were used in the calculation. Least squares calculation gave the best fit parameters of g_{Mn}, g_{Ni}, J_{MnNi}, J_{MnNi*}, J_{NiNi*}, and D being 1.915(5), 2.206(5), 4.5(1) cm^{-1}, 4.3(1) cm^{-1}, −7.9(2) cm^{-1}, and −0.85(1) cm^{-1}, respectively, and simulation curves calculated using these parameters were in good agreement with the experimental data (Figure 2). The ground spin state is, therefore, $S = 6$, and the first excited state of $S = 5$ is above 5 K. In addition, the fit with all positive J values was inferior.
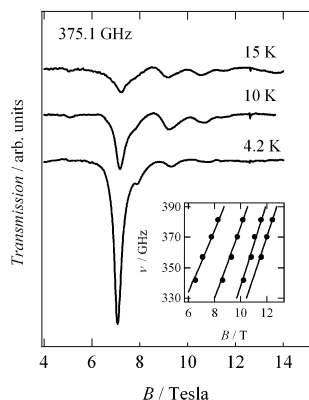
Figure 3. Selected high-field EPR spectra on single crystals of **1** measured at 375.1 GHz and plots of the field frequency versus resonance magnetic field for the observed peaks (inset). The applied magnetic field is tilted 48° with respect to the easy axis. Solid lines on the ν versus B plots result from a least-squares fit using the parameters described in the text.

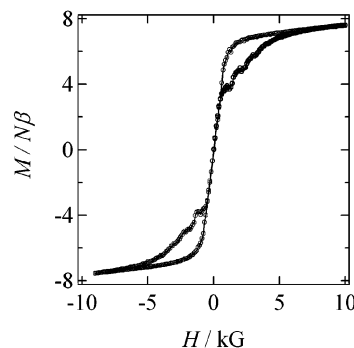**Figure 4.** Magnetization hysteresis loop for oriented crystals of **1** measured in an eicosane matrix at 0.55 K.

High-field EPR (HF-EPR) spectra for single crystals were collected at several frequencies (342−381 GHz) and temperatures (Figure 3). The spectrum at 4.2 K and a frequency of 375.1 GHz showed the most intense band at 7.05 T, and more fine structure was observed for the EPR signals at higher temperatures in the higher magnetic field region. This is due to the appreciable thermal energy needed to populate higher energy M_s levels, and the temperature dependence of the EPR signals indicates that **1** has a negative D value. In the crystal, two molecules are related by a 4-fold screw axis, and the equatorial coordination planes of the Mn^{III} ions make a dihedral angle of 89.68° to each other.[12] Each principal axis, which is along the apical axis of the Mn^{III} ion, is tilted to the external magnetic field. Using HF-EPR field frequency and resonance magnetic field data, D, g_{av}, and θ (the angle between the principal axis and external magnetic field) values were determined by the eigen field approach to be −0.70(1) cm^{-1}, 2.082(2), and 48.0(1)°, respectively (Figure 3 inset).[13]

1 possesses an $S = 6$ spin ground state with a negative D value, and it is, therefore, expected to be an SMM with a magnetization reversal barrier of $|D|S_z^2 = 36$ cm^{-1}. Magnetization experiments were carried out for oriented crystals in an eicosane matrix at 0.55 K, where the principal magnetic axis deviates from the external magnetic field, such as in the HF-EPR measurements. Magnetization data showed a steplike hysteresis loop, which proves that the molecule is an SMM (Figure 4).

We have found that tridentate Schiff bases and their reduced derivatives are versatile for assembling heterometal ions.[6g] It is hoped that through the chemical modification of the bridging ligands, molecules with a larger number of metal ions can be assembled and thus have higher-spin ground states and larger spin reversal barriers.

Supporting Information Available: Crystallographic details in CIF format and details of magnetic data analyses. This material is available free of charge via the Internet at http://pubs.acs.org.

References

(1) Christou, G.; Gatteschi, D.; Hendrickson, D. N.; Sessoli, R. *MRS Bull.* **2000**, *25*, 66.
(2) (a) Leuenberger, M. N.; Loss, D. *Nature* **2001**, *410*, 789. (b) Gatteschi, D.; Sessoli, R. *Angew. Chem., Int. Ed.* **2003**, *42*, 268. (c) Wernsdorfer, W.; Aliaga-Alcalde, N.; Hendrickson, D. N.; Christou, G. *Nature* **2002**, *416*, 406.
(3) (a) Sessoli, R.; Gatteschi, D.; Caneschi, A.; Novak, M. A. *Nature* **1993**, *365*, 141. (b) Sessoli, R.; Tsai, H.-L.; Schake, A. R.; Wang, S.; Vincent, J. B.; Folting, K.; Gatteschi, D.; Christou, G.; Hendrickson, D. N. *J. Am. Chem. Soc.* **1993**, *115*, 1804.
(4) (a) Castro, S. L.; Sun, Z.; Grant, C. M.; Bollinger, J. C.; Hendrickson, D. N.; Christou, G. *J. Am. Chem. Soc.* **1998**, *120*, 2365. (b) Aubin, S. M. J.; Wemple, M. W.; Adams, D. M.; Tsai, H.-L.; Christou, G.; Hendrickson, D. N. *J. Am. Chem. Soc.* **1996**, *118*, 7746. (c) Oshio, H.; Hoshino, N.; Ito, T. *J. Am. Chem. Soc.* **2000**, *122*, 12602. (d) Cadiou, C.; Murrie, M.; Paulsen, C.; Villar, V.; Wernsdorfer, W.; Winpenny, R. E. P. *Chem. Commun.* **2001**, 2666.
(5) (a) Aubin, S. M. J.; Dilley, N. R.; Pardi, L.; Krzystek, J.; Wemple, M. W.; Maple, M. B.; Brunel, L.-C.; Christou, G.; Hendrickson, D. N. *J. Am. Chem. Soc.* **1998**, *120*, 4991. (b) Barra, A. L.; Gatteschi, D.; Sessoli, R. *Chem.—Eur. J.* **2000**, *6*, 1608. (c) Friedman, J. R.; Sarachik, M. P.; Tejada, J.; Maciejewski, J.; Ziolo, R. *J. Appl. Phys.* **1996**, *79*, 6031.
(6) (a) Sokol, J. J.; Hee, A. G.; Long, J. R. *J. Am. Chem. Soc.* **2002**, *124*, 7656. (b) Osa, S.; Kido, T.; Matsumoto, N.; Re, N.; Pochaba, A.; Mrozinski, J. *J. Am. Chem. Soc.* **2004**, *126*, 420. (c) Zaleski, C. M.; Depperman, E. C.; Kampf, J. W.; Kirk, M. L.; Pecoraro, V. L. *Angew. Chem., Int. Ed.* **2004**, *43*, 3912. (d) Schelter, E. J.; Prosvirin, A. V.; Dumber, K. R. *J. Am. Chem. Soc.* **2004**, *126*, 15004. (e) Mishra, A.; Wernsdorfer, W.; Abboud, K. A.; Christou, G. *J. Am. Chem. Soc.* **2004**, *126*, 15648. (f) Choi, H. J.; Sokol, J. J.; Long, J. R. *Inorg. Chem.* **2004**, *43*, 1607. (g) Oshio, H.; Nihei, M.; Yoshida, A.; Nojiri, H.; Nakano, M.; Yamaguchi, A.; Karaki, Y.; Ishimoto, H. *Chem.—Eur. J.* **2004**, *11*, 843.
(7) Xie, Y.; Jiang, H.; Chang, A. S.; Liu, Q.; Xu, X.; Du, C.; Zhy, Y. *Inorg. Chim. Acta* **2002**, *333*, 138.
(8) A pale yellow methanol solution (10 mL) of MnCl$_2$·4H$_2$O (198 mg, 1.0 mmol), H$_2$salpa (199 mg, 1.0 mmol), and Et$_3$N (202 mg, 2.0 mmol) turned brown by air oxidation and was added to a methanol solution [10 mL of NiCl$_2$·6H$_2$O (237 mg, 1.0 mmol), H$_2$salpa (199 mg, 1.0 mmol), and Et$_3$N (202 mg, 2.0 mmol)]. After diethyl ether (5 mL) was added and the resulting mixture stored for 1 week, dark-red blocks were collected by filtration. Anal. Calcd (found) for C$_{40}$H$_{52}$Cl$_2$Mn$_2$N$_4$Ni$_2$O$_8$: C, 47.33 (47.08); H, 5.16 (5.31); N, 5.52 (5.34); Mn, 10.82 (10.56); Ni, 11.56 (11.32).
(9) Crystal data for **1**: C$_{40}$H$_{52}$Cl$_2$Mn$_2$N$_4$Ni$_2$O$_8$, 1015.06 g mol^{-1}, tetragonal $I4_1/a$, $a = 25.985(3)$ Å, $c = 13.169(2)$ Å, $V = 8891(2)$ Å^3, $Z = 8$, $T = 240$ K. Final $R1 = 0.0548$ and $wR2 = 0.143$ ($I > 2\sigma I$).
(10) Bond valence sums for the Mn^{III} and Ni^{II} ions of **1** were 2.928 and 2.043, respectively. (a) Brown, I.; Altermatt, D. *Acta Crystallogr.* **1985**, *B41*, 244. (b) Liu, W.; Thorp, H. H. *Inorg. Chem.* **1993**, *32*, 4102.
(11) $H = -2J_{MnNi}(S_{Mn}S_{Ni} + S_{Mn*}S_{Ni*}) - 2J_{MnNi*}(S_{Mn}S_{Ni*} + S_{Mn*}S_{Ni}) - 2J_{NiNi*}S_{Ni}S_{Ni*} + H_{zfs} + H_{Zeeman}$. Details of the magnetic data analyses are in the Supporting Information.
(12) Single crystals in the HF-EPR measurements were aligned by the strong external magnetic field.
(13) Belford, B. B.; Belford, R. L.; Burkhalter, J. F. *J. Magn. Reson.* **1973**, *11*, 251. The contribution of the biaxial anisotropy was ignored.

JA042217P